

Green Chemistry

Accepted Manuscript



This article can be cited before page numbers have been issued, to do this please use: S. Mincke, T. G. Asere, I. Verheye, K. Folens, F. Vanden Bussche, L. Lapeire, K. Verbeken, P. Van Der Voort, D. A. Tessema, F. Fufa, G. Dulaing and C. V. Stevens, *Green Chem.*, 2019, DOI: 10.1039/C9GC00166B.



This is an Accepted Manuscript, which has been through the Royal Society of Chemistry peer review process and has been accepted for publication.

Accepted Manuscripts are published online shortly after acceptance, before technical editing, formatting and proof reading. Using this free service, authors can make their results available to the community, in citable form, before we publish the edited article. We will replace this Accepted Manuscript with the edited and formatted Advance Article as soon as it is available.

You can find more information about Accepted Manuscripts in the [author guidelines](#).

Please note that technical editing may introduce minor changes to the text and/or graphics, which may alter content. The journal's standard [Terms & Conditions](#) and the ethical guidelines, outlined in our [author and reviewer resource centre](#), still apply. In no event shall the Royal Society of Chemistry be held responsible for any errors or omissions in this Accepted Manuscript or any consequences arising from the use of any information it contains.

Functionalized chitosan adsorbents allow recovery of palladium and platinum from acidic aqueous solutions

Stein Mincke,^{*a} Tsegaye Grima Asere,^{*b,c} Ivar Verheye,^a Karel Folens,^a Flore Vanden Bussche,^{a,d} Linsey Lapeire,^e Kim Verbeken,^e Pascal Van Der Voort,^d Dejene A. Tessema,^b Fekadu Fufa,^c Gijs Du Laing^a and Christian V. Stevens^a

Received 00th January 20xx,
Accepted 00th January 20xx

DOI: 10.1039/x0xx00000x

www.rsc.org/

Platinum (Pt) and palladium (Pd) are precious metals considered critical in our society and needed in a variety of sustainable technologies. Their scarcity urges to increase the recycling from secondary waste streams through new and efficient recovery techniques. Adsorption is an established recovery method for liquid streams, where chitosan shows promising results as a low-cost adsorbent, derived from biomass. This biopolymer is able to capture metals, but suffers from a low stability in acidic conditions and poor adsorbing properties. In this study, three new chitosan derivatives were synthesized and employed for Pd(II) and Pt(IV) recovery from acidic solutions. Specific and simple modifications were selected based on known affinities for these metal ions and taken into account the principles of green chemistry. The prepared derivatives consist of 1,10-phenanthroline-2,9-dicarbaldehyde cross-linked chitosan (Ch-PDC), [2,2'-bipyridine]-5,5'-dicarbaldehyde cross-linked chitosan (Ch-BPDC) and glutaraldehyde cross-linked chitosan grafted with 8-hydroxyquinoline-2-carbaldehyde (Ch-GA-HQC). For all derivatives, the adsorption was very fast and equilibrium reached within 30 min. The Langmuir isotherms revealed a maximum adsorption capacity for Pd(II) and Pt(IV) of respectively 262.6 mg/g and 119.5 mg/g for Ch-PDC, 154.7 mg/g and 98.3 mg/g for Ch-BPDC and 340.3 mg/g and 203.9 mg/g for Ch-GA-HQC. Such adsorption capacities are considerably higher compared to biosorbents reported in literature. Excellent physical properties in homo- and heterogeneous systems and high regeneration performances demonstrate that chitosan-based adsorbents are very promising for Pd(II) and Pt(IV) recovery from acidic solutions.

Introduction

The introduction of the Sustainable Development Goals in 2015 gave a renewed attention to the long-term care for planet Earth and its inhabitants. Concepts of circular economy and sustainable technologies substantiate these goals in the processing industries, where the reduction and valorization of waste are central. In this context, chitosan has been widely studied, since it is sourced from waste streams and applied as building block for added value materials. Chitosan is a polymer of biological origin, consisting of randomly distributed D-glucosamine and *N*-acetyl-D-glucosamine units, linked through a $\beta(1\rightarrow4)$ bond. It is mainly obtained from chitin after *N*-deacetylation under basic conditions (Fig. 1).^{1–3} Chitin is the

second most abundant natural biopolymer and can be found as a structural component in the exoskeleton of arthropods such as crustaceans or insects, or in the cell wall of yeast and fungi.^{2,4} For that matter, the entorefinery concept is an emerging biorefinery approach where insects are used to convert organic and food waste into biodiesel, useful proteins and chitin.^{5–7}

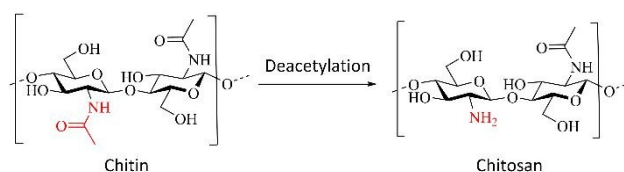


Fig. 1 Structures of chitin and chitosan¹

The unique chemical and biological properties of chitosan, *e.g.* biocompatibility, bioactivity and biodegradability, are valued in many fields.^{1,8–10} For example, chitosan is used for the adsorption of metals in wastewater treatment. Biosorption can be considered as an effective and sustainable process in comparison to conventional metal recovery techniques, since cheap chitinous materials, algal biomass or microbial biomass can be used.^{11–13} The use of biosorbents in the recovery of platinum group metals (PGM) from waste streams is of particular interest for the processing industries. The PGMs are a group of six noble elements (Ru, Rh, Pd, Os, Ir and Pt) that are regarded as precious metals. They have similar physical and

^a SynBioC research group, Department of Green Chemistry and Technology, Ghent University, Campus Coupure, Coupure Links 653, 9000 Ghent, Belgium

^b Department of Chemistry, Welkite University, Gubrei Wabe Bridge 5, Southern Nations, Nationalities and Peoples' Region, Welkite, Ethiopia

^c Department of Water Resources and Environmental Engineering, Jimma University, P.O. Box 378, Jimma, Ethiopia

^d Department of Chemistry, Ghent University, Krijgslaan 281 S3, 9000 Ghent, Belgium

^e Department of Materials, Textiles and Chemical Engineering, Ghent University, Technologiepark Zwijnaarde 46, 9052 Zwijnaarde, Belgium

*These authors made equivalent contributions

†Electronic Supplementary Information (ESI) available. See

DOI: 10.1039/x0xx00000x

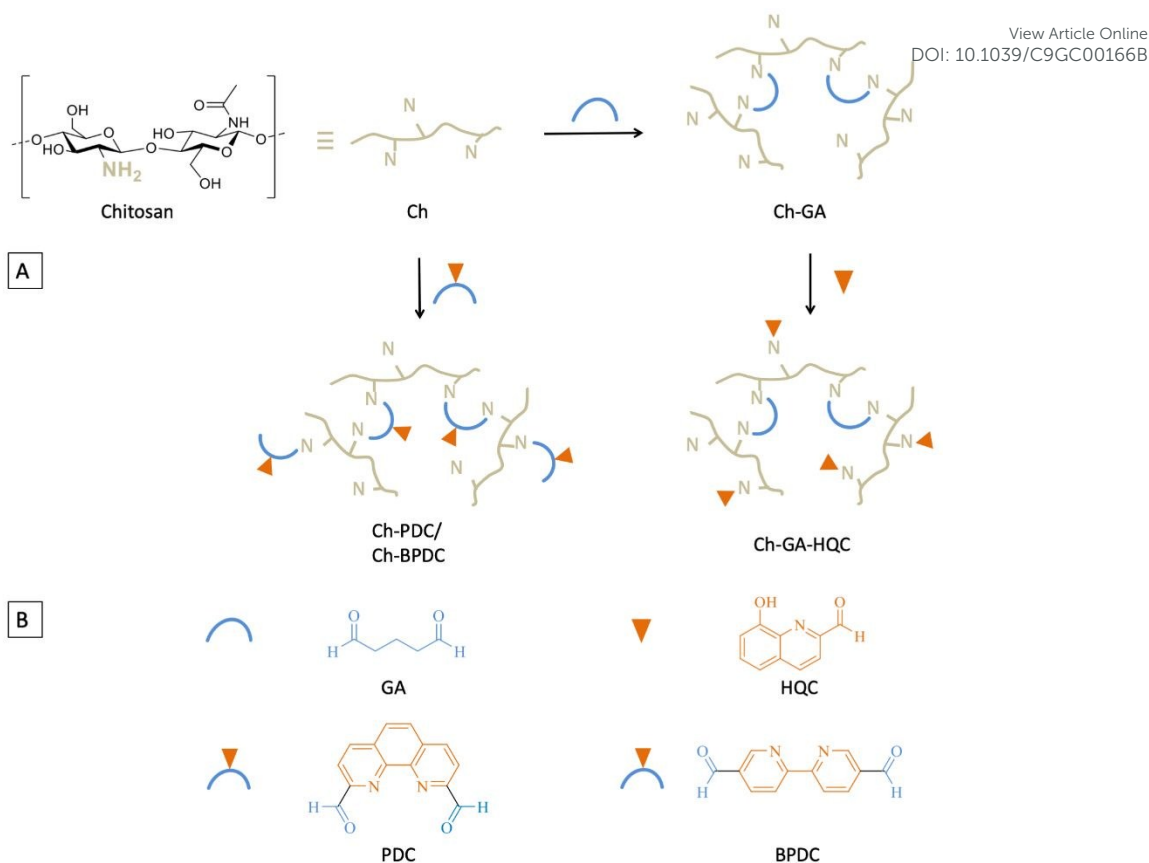


Fig. 2 Schematic overview of the synthesis of Ch-PDC, Ch-BPDC and Ch-GA-HQC (A) and the chelating and cross-linking compounds (B)

chemical properties which are desirable in a variety of modern applications.^{14,15} Palladium (Pd) and platinum (Pt) are used in sustainable technologies, such as fuel cells, catalysts in vehicles, petrochemical conversion processes and electronics. Despite the wide scope of applications, the natural availability of Pt and Pd is limited and, hence, they belong to the most expensive resources. To move towards a sustainable society, these critical metals should be recovered from waste streams and used again as a secondary source of raw materials.^{15–20}

The use of chitosan as biosorbent for Pd and Pt adsorption first requires chemical modification since native chitosan lacks stability at low pH and has only moderate adsorption capacities towards metal ions.^{21–23} To increase the stability at low pH, cross-linking of the polymer with di/polyfunctional reagents is commonly used. In this respect, glutaraldehyde is by far the most studied cross-linking agent, amongst many other possibilities.^{24–29} Attention should be paid to the type and degree of cross-linking, together with the cross-linking conditions, since these parameters affect the adsorption capacity.^{24,30,31}

This study focuses on the synthesis of acid-tolerant and high-performance chitosan-based sorbents, able to recover Pd(II) and Pt(IV) from aqueous media. Native chitosan was derivatized under homogeneous conditions via a simple one- or two-step modification involving cross-linking and the addition of a metal chelating moiety. Three different biosorbents are synthesized

and characterized using Secondary Electron Microscopy (SEM), Fourier Transform Infrared (FTIR) spectroscopy, Thermogravimetric analysis (TGA), X-ray powder diffraction (XRPD) analysis, elemental analysis and Brunauer-Emmett-Teller (BET) surface area analysis. The adsorption and kinetic performances were studied together with the effect of the pH and selectivity towards the metal ions. Furthermore, the regeneration of the derivatives was investigated, indicating their reusability.

Results and discussion

Synthesis and characterization of chitosan derivatives

Chitosan was modified to reduce the acid solubility and to increase the number of metal sorption sites (Fig. 2A). Therefore, chitosan (Ch) was dissolved in a 1% acetic acid solution and derivatized with 1,10-phenanthroline-2,9-dicarbaldehyde (PDC), [2,2'-bipyridine]-5,5'-dicarbaldehyde (BPDC), or 8-hydroxyquinoline-2-carbaldehyde (HQC) (Fig. 2B). These particular compounds were selected for their known affinity towards Pd and Pt species.^{32–35} Since HQC is not able to cross-link chitosan, glutaraldehyde (GA) was added prior to the addition of HQC. The amount of cross-linker added was based on previous optimization experiments available in literature.³⁶ The formed imine bonds were reduced to secondary amines. An increase of the viscosity was clearly visible after the addition of the cross-linking agents, indicating efficient cross-linking. The resulting chitosan derivatives (Ch-PDC, Ch-BPDC and Ch-GA-

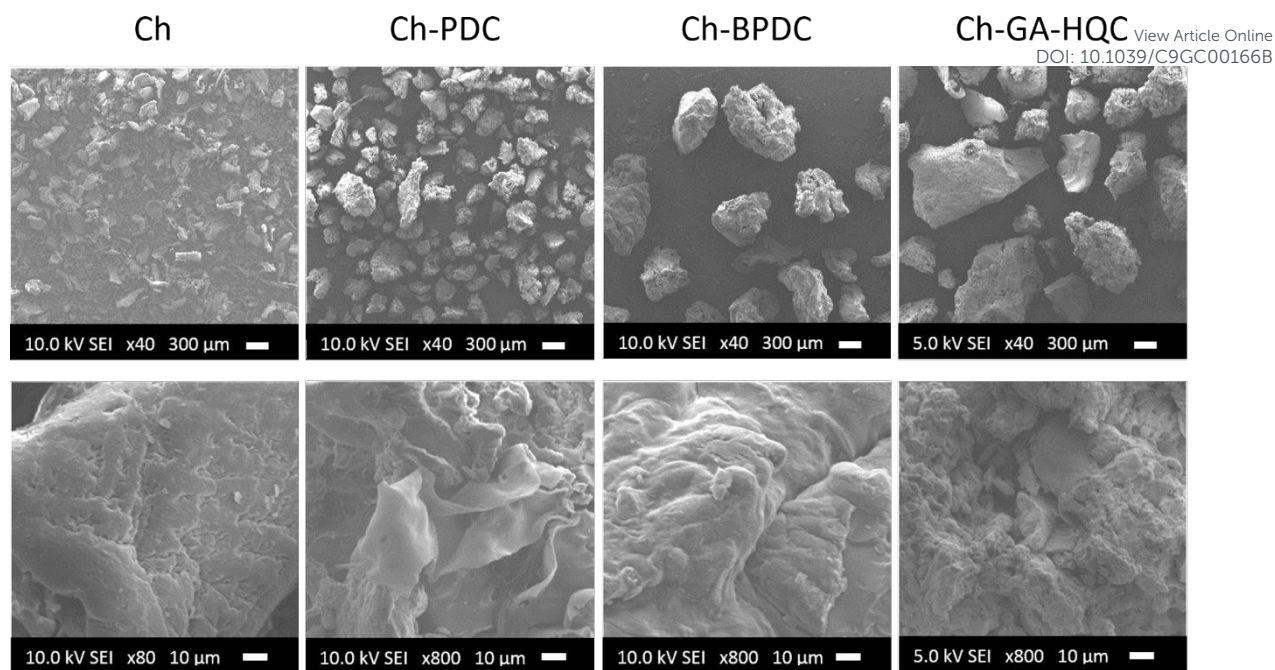


Fig. 3 Secondary electron (SE) images from native chitosan (Ch) and chitosan derivatives (Ch-PDC, Ch-BPDC and Ch-GA-HQC) at different magnifications

HQC) were investigated by SEM, FTIR-spectroscopy, XRPD and TGA. Further characterization results (elemental analysis and BET surface area) can be found in supporting information.

From the secondary electron (SE) images, it is clear that the native chitosan flakes (Ch) are the smallest compared to the modified samples (Fig. 3). The difference is explained by the addition of a cross-linker, that bridges the chains resulting in larger entities. The Ch-PDC particles appear to be smaller compared to those of Ch-BPDC and Ch-GA-HQC. At higher magnifications, all chitosan derivatives have a higher surface roughness in comparison with the native chitosan, which has a smoother surface.

The FTIR-spectra of all derivatives show a single broad peak around 3300 cm^{-1} , compared to two peaks at 3354 cm^{-1} and 3288 cm^{-1} for chitosan (Fig. 4).³⁷ The two peaks for chitosan indicate N-H stretching of primary amines (and O-H stretching),

whereas the single broad peak indicates N-H stretching of secondary amines as a result of cross-linking and/or grafting. Additionally, the peak(s) at 856 cm^{-1} for Ch-PDC, 835 cm^{-1} , 752 cm^{-1} and 717 cm^{-1} for Ch-BPDC and 819 cm^{-1} and 742 cm^{-1} for Ch-GA-HQC indicate the presence of an aromatic system, corresponding to the phenanthroline, bipyridine and quinoline moiety respectively. The sharp peaks at 2981 cm^{-1} and 1381 cm^{-1} in the spectrum of Ch-GA-HQC correspond to C-H vibration, coming from the CH_2 cross-linking unit of glutaraldehyde. A detailed peak assignment is given in the supporting information. XRPD analysis was performed to investigate the changes in structural organization by the modification of chitosan. XRPD results of native chitosan (A) and the modified sorbents (B, C and D) are depicted in Fig. 5 and clearly show the amorphous nature of these materials. The characteristic diffraction peak of chitosan was observed at 20° in all spectra.³⁷ However, the use of a cross-linking unit lowers the intensity of

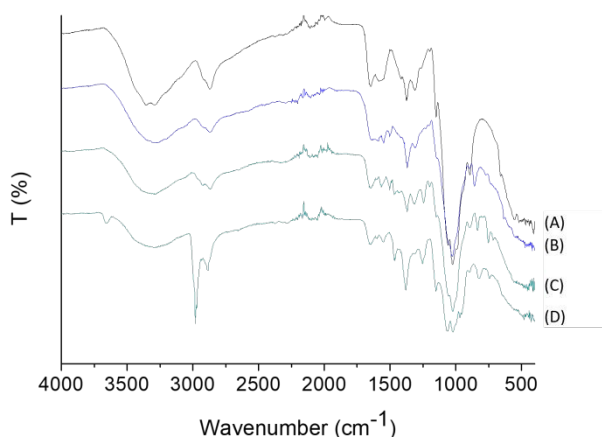


Fig. 4 FTIR spectra of chitosan (A) and chitosan derivatives Ch-PDC (B), Ch-BPDC (C) and Ch-GA-HQC (D)

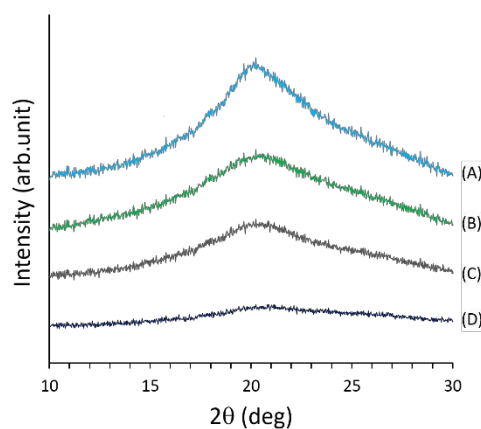


Fig. 5 XRPD spectra of chitosan (A), Ch-PDC (B), Ch-BPDC (C) and Ch-GA-HQC (D)

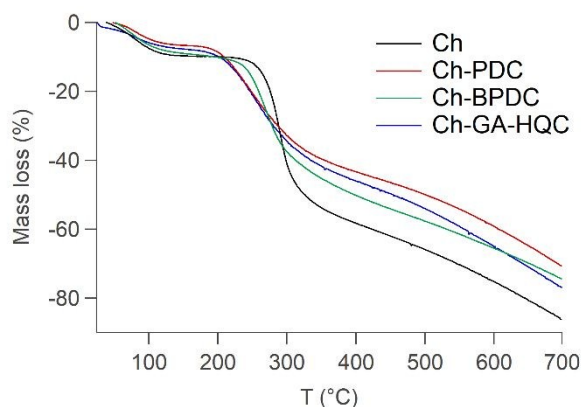


Fig. 6 TG curves of the thermal degradation of chitosan and chitosan derivatives

this peak, which indicates a loss in the structural organization. This is a result of the cleavage of hydrogen bonds that organize the supramolecular structure of the polysaccharide chains.^{38,39} In the case of Ch-GA-HQC (D), two compounds (GA and HQC) cause structural changes, resulting in a lower peak intensity compared to (B) and (C).

Thermogravimetric analysis was performed to investigate the effect of cross-linking on the temperature profile of the materials (Fig. 6). Native chitosan shows a well-defined decomposition at 300 °C.^{40,41} The decomposition of all cross-linked derivatives, on the other hand, starts at a lower temperature (200 °C) and proceeds within a broader temperature profile. At high temperatures, more residual tar remains for these cross-linked derivatives. Therefore, it is clear that cross-linking has a significant effect on the thermal stability of chitosan. All results mentioned above indicate a successful reaction of chitosan with the chelating and cross-linking compounds PDC, BPDC and GA-HQC.

Effect of initial pH

The effect of pH on the adsorption of Pt(IV) and Pd(II) was investigated in separate solutions using the three chitosan derivatives. The pH was varied between 1 and 5 since most wastewater streams are acidic, e.g. from acid-leachate of

catalytic converters. These waste streams contain only low concentrations of precious metals (10–40 mg/L), therefore an initial element concentration of 25 mg/L was used.

To study the effect of pH on the adsorption capacity, the metal speciation and the point of zero charge (pH_{PZC}) of the chitosan derivatives were investigated. The point of zero charge (pH_{PZC}) is considered an important parameter when studying the effect of pH on the adsorption capacity of materials. Chitosan is reported to have a pH_{PZC} of 6.3, in which the protonation of the available amine groups plays an important role.⁴³ For the modifications performed in this study, the amine groups were used in order to functionalize and cross-link chitosan. The pH_{PZC} of the biosorbents was determined and can be found in the supporting information. All pH_{PZC} values (3.7–4.7) are well in the pH 1–5 range.

For Pd, all derivatives show a slightly increased adsorption efficiency when the pH increases from 1 to 5 (Fig. 7). The adsorption capacity is not much affected when the pH rises above the pH_{PZC} of the materials. This can be ascribed to the occurrence of different adsorption mechanisms. Adsorption can occur through electrostatic attraction between negatively charged metal species and positively charged amine groups ($pH < pH_{PZC}$)^{44–46} or through coordination of the amine and hydroxyl groups with the metal species ($pH > pH_{PZC}$).^{39,47} By increasing the pH from 1 to 5, a slight increase of the adsorption capacity for Pd can be attributed to a slightly better coordination interaction compared to electrostatic attractions. Besides the pH_{PZC} , the governing speciation of the metal species also affects the adsorption. The type of speciation is highly determined by the pH of the solution and concentration of chloride ions present during adsorption. Speciation modelling is often used in literature to investigate the type of speciation of the metal species.^{48,49} Accordingly, $PdCl_4^{2-}$ is considered to be the predominant species at all pH levels used in the experiments.⁵⁰ The increase in adsorption efficiency, as the pH increases from 1 to 5, can be related to a reduced competition between chloride ions and $PdCl_4^{2-}$ at higher pH levels. At low pH levels, the attraction of counter anions, such as chloride, towards positively charged adsorbents is stronger and involves competition with $PdCl_4^{2-}$.³⁶

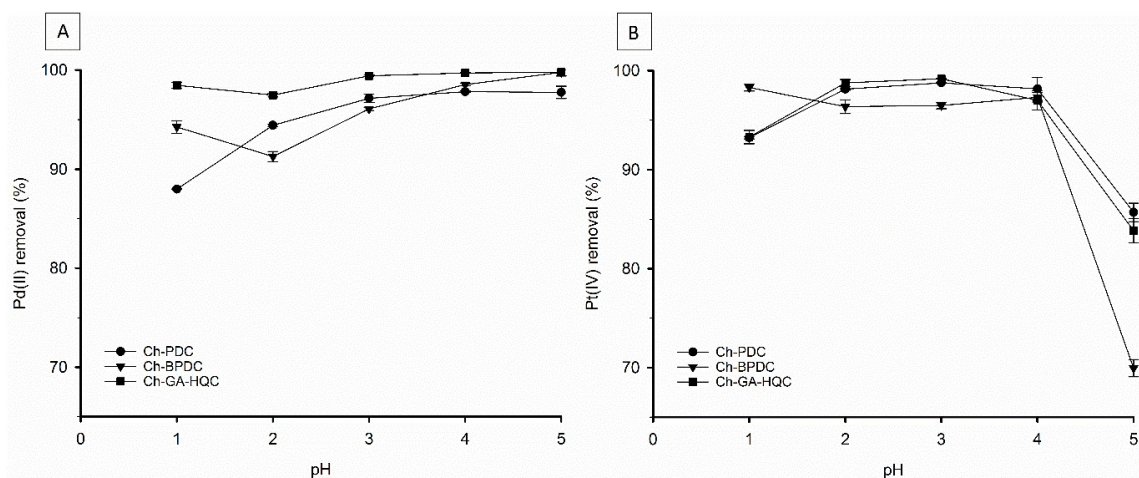


Fig. 7 pH effect on removal of Pd(A) and Pt(B) using Ch-PDC, Ch-BPDC or Ch-GA-HQC adsorbents

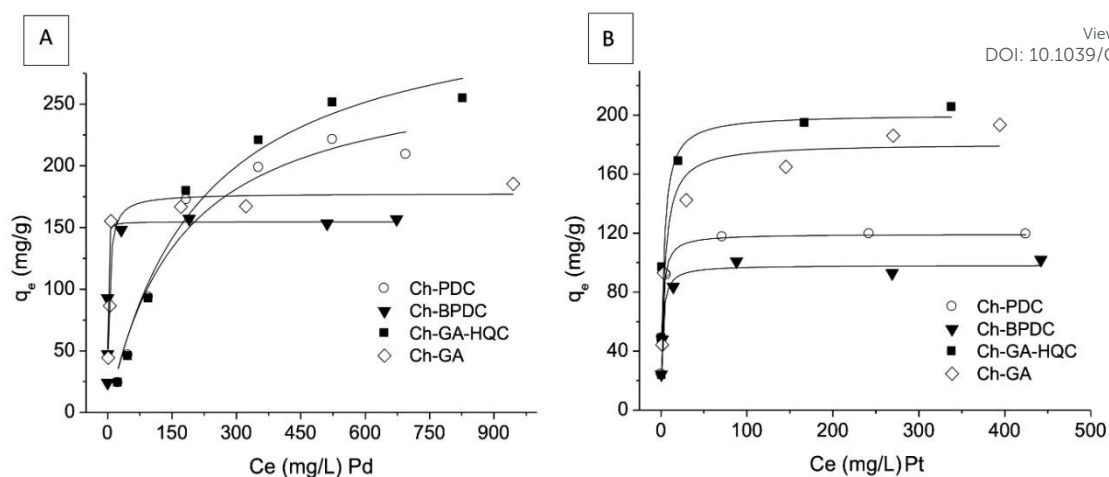


Fig. 8 Langmuir adsorption isotherms of Pd (A) and Pt (B) on Ch-PDC, Ch-BPDC, Ch-GA-HQC and Ch-GA

In contrast to what is observed for Pd, the removal efficiency of Pt rises when the pH is increased from 1 to 4, but decreases again if the pH is further increased to pH 5. Fujiwara et al.⁵¹ also reported that higher adsorption capacity of lysine modified chitosan for precious metal ions was obtained at pH 1 – 4. The drop in sorption capacity occurs when the pH rises above the pH_{PZC} . In this respect, electrostatic attraction is considered the dominant adsorption mechanism. Furthermore, it is important to notice that Pt can be present as chloro-complex, because hydrochloric acid was used in the preparation of the adsorbate solutions. The distribution of these complexes depends on pH, chloride concentration and metal concentration. At pH 1 – 5.5, Pt is mainly present as $PtCl_6^{2-}$ and from pH 5.5 to 8, $PtCl_5(OH)^2-$ is expected to be the dominant species.^{50,52} At pH 1, the interaction between the excess chloride ions and the positively charged adsorbents increased, resulting in a greater competition between chloride ions and hexachloroplatinate. At pH 5, *i.e.* closer to the pH_{PZC} of the adsorbents, electrostatic interactions become less pronounced and the recovery efficiency decreases. Hence, pH 3 was selected for further adsorption experiments. The suggested removal mechanism at this pH is mainly based on ion-exchange onto protonated nitrogen groups of the chitosan-based sorbents.⁵¹ Moreover, performing the adsorption at a low pH value is an important strategy to obtain selectivity in adsorption away from base metal ions.⁵³

Adsorption isotherms

Figure 8 shows the adsorption isotherms of Pd and Pt, on the synthesized chitosan derivatives (Ch-PDC, Ch-BPDC, Ch-GA-HQC and Ch-GA). The parameters resulting from fitting the experimental data to the Langmuir model are presented in Table 1. The value of q_m (obtained from Langmuir plots) is consistent with the experimental results, indicating that the adsorption of Pd(II) and Pt(IV) onto Ch-PDC, Ch-BPDC and Ch-GA-HQC occurs through a monolayer deposition.^{44,54} The adsorption capacity for Pd was found to increase in the order Ch-BPDC < Ch-PDC < Ch-GA-HQC. Additional functionalization of Ch-GA by 8-hydroxyquinoline-2-carbaldehyde (HQC) ameliorated the Pd adsorption capacity from 177.7 mg/g to 340.3 mg/g. Similar adsorption capacities for Ch-GA were reported in literature.^{36,55} Also for Pt adsorption, an increase was observed through the addition of HQC to Ch-GA, namely from 180.8 mg/g to 203.9 mg/g. Although the adsorption capacity of Pt is in general lower than that of Pd, the same order of materials performance counts. The preference of Pd(II) adsorption over Pt(IV) was reported earlier for several chitosan-based adsorbents.^{56,57} Wang et al.⁵⁸ also reported the greater adsorption potential of Pd(II) over Pt(IV) on alginate and algal-based beads at pH 2.5 in a mono-component system. The difference in the observed adsorption capacities can be associated with the difference in the affinity of the adsorbents towards these metals.⁴⁸ The highest Pd(II) and Pt(IV) adsorption capacity is obtained by Ch-GA-HQC, compared to Ch-PDC and

Table 1 Parameters of adsorption isotherms for Pt(IV) and Pd(II) adsorption onto the synthesized chitosan derivatives for the Langmuir model with standard error (SE)

Element	Parameter	Ch-PDC (SE)	Ch-BPDC (SE)	Ch-GA-HQC (SE)	Ch-GA (SE)
Pd	q_m (mg/g)	262.6 (21.4)	154.7 (9.0)	340.3 (29.9)	177.7 (7.8)
	K_L (L/mg)	0.006 (0.002)	3.53 (1.01)	0.005 (0.001)	0.29 (0.08)
	R_L	0.169 - 0.873	0.0003 - 0.012	0.204 - 0.896	0.004 - 0.713
	R^2	0.9538	0.8999	0.9695	0.8695
Pt	q_m (mg/g)	119.5 (2.8)	98.3 (2.3)	203.9 (10.5)	180.8 (5.6)
	K_L (L/mg)	0.62 (0.12)	0.61 (0.12)	0.33 (0.10)	0.20 (0.11)
	R_L	0.002 - 0.061	0.002 - 0.063	0.004 - 0.108	0.01 - 0.727
	R^2	0.9974	0.9775	0.8877	0.9385

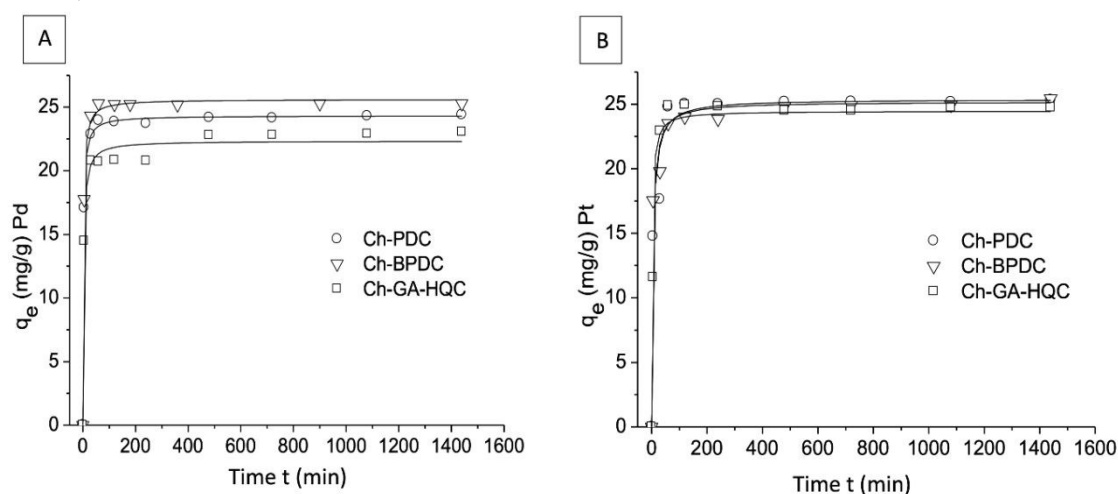
Table 2 Comparison of adsorption capacities of cross-linked chitosan compoundsView Article Online
DOI: 10.1039/C9GC00166B

Adsorbent	pH	Adsorption capacity (mg/g)		Reference
		Pd(II)	Pt(IV)	
Chitosan flakes	2	62.5	66.6	[60]
L-lysine modified cross-linked chitosan resin	1, 2	109.5	129.3	[51]
Chitosan cross-linked hydrogels	2	192.9	231.1	[56]
Glycine modified cross-linked chitosan resin	2	120.4	122.5	[61]
Thiourea modified chitosan microspheres	2	112.4	129.9	[45]
Ethylenediamine-modified magnetic chitosan nanoparticles	2	138	171	[44]
Azacrown ether cross-linked chitosan	4	173.1	-	[62]
Rubanic acid grafted cross-linked chitosan	2	352.0	-	[63]
2-aminobenzaldehyde modified chitosan	5	275	-	[39]
β -cyclodextrin grafted chitosan	6	202.0	-	[64]
Azobenzene modified chitosan	4.1	101.6	-	[65]
Glutaraldehyde cross-linked chitosan	2	204.7	-	[36]
Glutaraldehyde cross-linked chitosan	8	166.7	-	[55]
Glutaraldehyde cross-linked chitosan	3	177.7	180.8	This study
Sulphur-modified chitosan	2.5	38.5	-	[66]
Cross-linked sulfoethylated chitosan	2	42.6	-	[67]
Glutaraldehyde cross-linked chitosan	2	-	300	[68]
Polyethyleneimine-loaded core-shell chitosan beads	1	-	815.2	[69]
Ch-PDC	3	282.6	119.5	This study
Ch-BPDC	3	154.7	98.3	This study
Ch-GA-HQC	3	340.3	203.9	This study

Ch-BPDC. This could be ascribed to the difference in the synthesis process. In the case of Ch-PDC and Ch-BPDC, the addition of one compound (PDC and BPDC, respectively) causes both cross-linking and an increase in adsorption sites. In the case of Ch-GA-HQC, two separate compounds are used. Namely, cross-linking is obtained by glutaraldehyde, whereas HQC increases the sorption capacity. For all derivatives, the feasibility of the adsorption system could be evaluated by calculating the separation factor R_L . All R_L values for Pd and Pt adsorption are in between zero and one, indicating that the adsorption of both precious metals is favourable and irreversible.⁵⁹

Table 2 shows the comparison of the adsorption capacity of Ch-PDC, Ch-BPDC and Ch-GA-HQC for Pt(IV) and Pd(II) as a benchmark towards other chitosan-based adsorbents. Few studies examined both the adsorption of Pd and Pt. In this respect, Ch-GA-HQC is the best chitosan-based adsorbent

available. The Pd adsorption capacity of the synthesised chitosan derivatives were higher or at least comparable to earlier reports. Only rubanic acid chitosan derivatives (352 mg/g) were slightly better than Ch-GA-HQC (340.3 mg/g). Note that the pH was not the same in both studies and that the adsorption capacity of rubanic acid modified chitosan derivatives was strongly influenced by the pH. The Pt adsorption capacity of the derivatives from this study were comparable to other chitosan-based adsorbents. Polyethyleneimine-loaded chitosan beads showed the highest adsorption capacity for Pt. The high adsorption can be mainly attributed to the presence of the polyethyleneimine at the surface of the beads, since chitosan was only present in the core.⁶⁹ Generally, cross-linking chitosan and modifying it with nitrogen- and sulphur-containing groups significantly enhanced the Pd(II) and Pt(IV) adsorption capacity of chitosan in acidic solutions.

**Fig. 9** Plots of pseudo-second-order fit for Pd (A) and Pt (B) adsorption on Ch-PDC, Ch-BPDC and Ch-GA-HQC

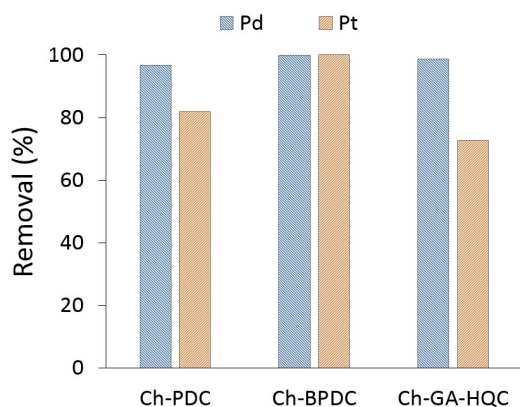


Fig. 10 Concomitant removal (%) of 25 mg L⁻¹ Pd and 25 mg L⁻¹ Pt by Ch-PDC, Ch-BPDC and Ch-GA-HQC

Adsorption kinetics

In order to investigate the adsorption rate, the effect of contact time was investigated at pH 3 using Ch-PDC, Ch-BPDC and Ch-GA-HQC adsorbents. The results of kinetic studies are shown in Fig. 9. The kinetic curve for Pd and Pt showed a rapid adsorption within the first 30 min. The equilibrium was reached in 120 min. The high adsorption rate in the beginning is due to the abundant active sites on the external surface of the adsorbent, available for interaction with Pd or Pt. The adsorption process slows down between 30 and 120 min. The experimental data were fitted with a non-linear pseudo-first-order (supporting information) and pseudo-second-order kinetic model. Since the pseudo-second-order fitting gave higher correlation coefficients, only these results are described here (Table 3). The excellent fit of the pseudo-second-order model suggests that the main adsorption mechanism is chemisorption. A similar phenomenon was observed in the adsorption of Pd(II) on cysteine functionalized 2,3-dialdehyde cellulose,⁷⁰ Pd(II) on glutaraldehyde cross-linked chitosan,⁵⁵ Pt(IV) on chitosan and Au(III), Pt(IV) and Pd(II) onto glycine modified cross-linked chitosan resin.^{23,61} The calculated adsorption rates k_2 were high for Pd (0.016 – 0.020 g/mg.min) and Pt (0.008 – 0.017 g/mg.min). Differences in k_2 values can be attributed to a different molecular geometry of both elements. In a mixed system, slightly higher adsorption rates for Pd are reflected in a relatively larger adsorption compared to Pt (Fig. 10), illustrating that adsorption in the presence of multiple compounds is kinetically controlled. For Pd, the value of k_2 increases in the order of Ch-GA-HQC < Ch-BPDC < Ch-PDC, whereas Ch-GA-HQC < Ch-PDC < Ch-BPDC for Pt. The intra-particle diffusion model

was employed to determine if pore diffusion or internal diffusion is the rate-determining step in the adsorption process. If the sole rate-limiting step is pore or intra-particle diffusion, the plot of q_t vs $t^{0.5}$ should be a straight line, passing through the origin.⁶¹ However, it is observed from Fig. 11 that the data are multi-linear and lines are not passing through the origin. The multi-linear trend indicates two steps in the sorption process: an initial linear phase due to external mass transfer, versus a later linear phase due to intra-particle diffusion.⁷¹ Immediately after mixing the adsorbent, bulk diffusion is the rate limiting factor, which may be related to a limited BET surface area (≤ 2 m²/g) of the materials. (Analysis results in supporting information). Similar observations were found by the adsorption of Au(III), Pt(IV) and Pd(II) onto glycine modified cross-linked chitosan resins,⁶¹ and Pd(II) adsorption with soluble tannins cross-linked *Lagerstroemia speciosa* leaves powder.⁷¹

Table 3 Parameters of the pseudo-second-order kinetic model for Pd and Pt adsorption on Ch-PDC, Ch-BPDC and Ch-GA-HQC with standard error (SE)

Element	Parameter	Ch-PDC (SE)	Ch-BPDC (SE)	Ch-GA-HQC (SE)
Pd	$q_{e,exp}$ (mg/g)	24.2 (0.1)	25.2 (0.1)	22.8 (0.1)
	$q_{e,cal}$ (mg/g)	24.3 (0.1)	25.6 (0.1)	22.4 (0.3)
	k_2 (g/(mg.min))	0.020 (0.001)	0.018 (0.001)	0.016 (0.002)
	R^2	0.9991	0.9984	0.9881
Pt	$q_{e,exp}$ (mg/g)	25.0 (0.4)	24.8 (0.3)	24.8 (0.3)
	$q_{e,cal}$ (mg/g)	25.2 (0.6)	24.5 (0.5)	25.4 (0.4)
	k_2 (g/(mg.min))	0.009 (0.002)	0.017 (0.002)	0.008 (0.001)
	R^2	0.9574	0.9768	0.9885

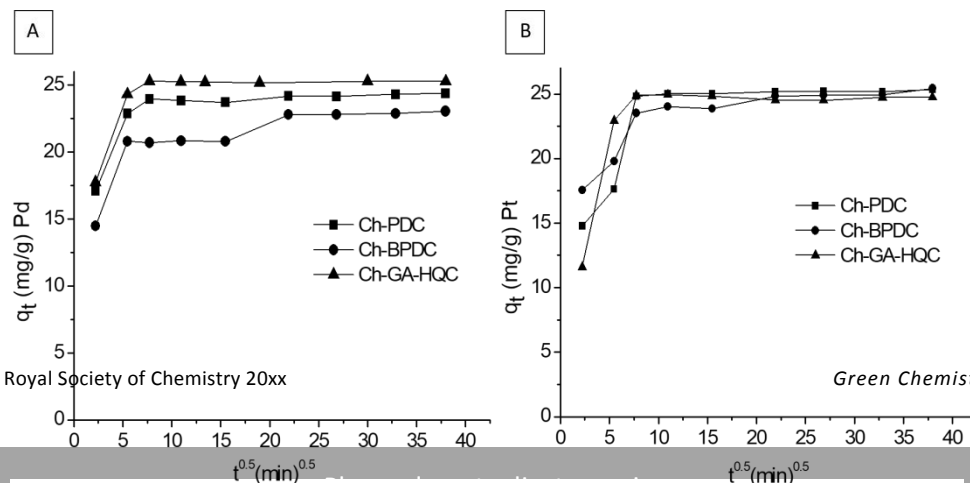


Fig. 11 Intra-particle diffusion plots of Pd (A) and Pt (B) adsorption on Ch-PDC, Ch-BPDC and Ch-GA-HQC

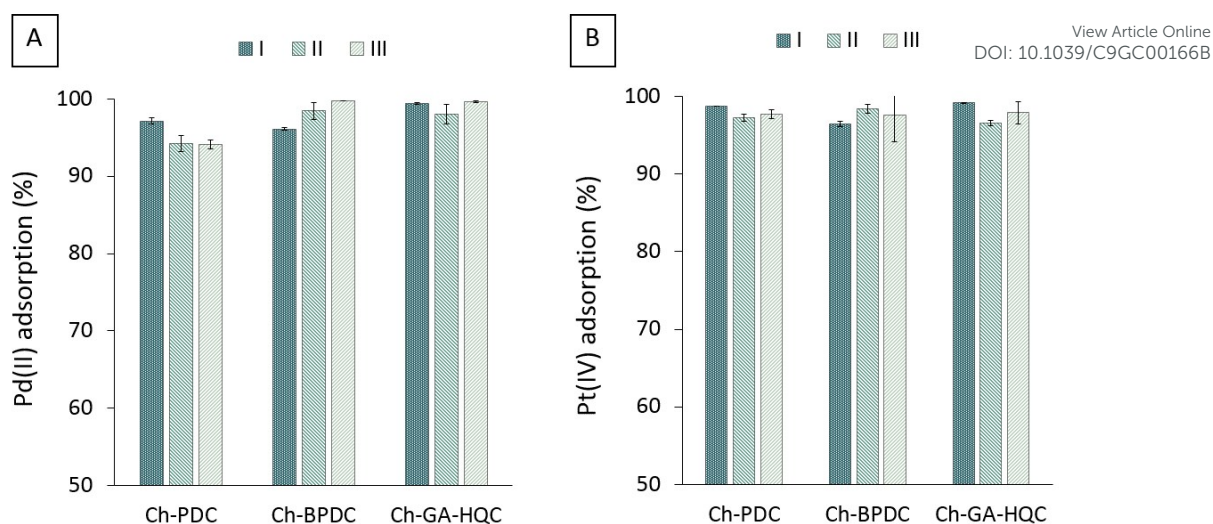


Fig. 12 Pd (A) and Pt (B) removal (%) in subsequent adsorption cycles (I, II and III) following desorption

Regeneration of biosorbents

After Pd or Pt adsorption onto the synthesized chitosan derivatives, the adsorbents were regenerated by using thiourea, a common and green reagent,⁷² under mild conditions and reused in subsequent adsorption cycles. The adsorption efficiencies of Pd(II) in the third cycle were 94.1% (Ch-PDC), 99.8% (Ch-BPDC) and 99.6% (Ch-GA-HQC). Those for Pt(IV) were 97.7% (Ch-PDC), 97.6% (Ch-BPDC) and 97.9% (Ch-GA-HQC) (Fig. 12). These values indicate that all three chitosan derivatives can be regenerated and reused for Pd(II) and Pt(IV) immobilization, adding to the successful application as adsorbents for resource recovery. The favourable regeneration allows the adsorbents to be packed in a column for continuous recovery of Pd and Pt from a liquid waste stream with intermittent regeneration.

Experimental

Materials

Precious metals used in this study are PdCl₂ (Merck, Darmstadt, Germany) and K₂PtCl₆ (Alfa Aesar, Thermo Fischer (kandel), GmbH, Germany). 5,5'-dimethyl-2,2'-bipyridine was purchased from TCI Europe (Zwijndrecht, Belgium) and solid thiourea (>99%) from Chem-Lab (Zedelgem, Belgium). Chitosan powder (low molecular weight, 75-85% deacetylated), together with all other chemicals, were supplied from Merck (Darmstadt, Germany). All these chemicals were of analytic grade or higher and used without further purification.

Synthesis and characterization of chelating and cross-linking compounds

Three metal chelating compounds were synthesized in a one- or two-step synthesis: 1,10-phenanthroline-2,9-dicarbaldehyde (PDC), [2,2'-bipyridine]-5,5'-dicarbaldehyde (BPDC) and 8-hydroxyquinoline-2-carbaldehyde (HQC) (Fig. 2B). The exact synthesis and characterization of these molecules can be found in the supporting information. The melting point was

determined using a Wagner & Munz Kofler Hot Bench (type WME). IR spectra with a S/N-ratio of 30,000:1 were obtained from samples in neat form with a Quest ATR (Attenuated Total Reflectance) accessory with diamond crystal puck using a Shimadzu IRAFFINITY-1S Fourier transform infrared spectrophotometer. All ¹H NMR spectra were recorded at 400 MHz, on a Bruker Avance III, equipped with 1H/BB z-gradient probe (BBO, 5 mm). CDCl₃ and DMSO-d₆ were used as solvent and TMS was used as an internal chemical shift standard. NMR spectra were acquired through the standard sequences available in the Bruker pulse program library and collected data processed using TOPSPIN 3.2.

Chitosan modification and characterization

Derivatization of chitosan with PDC or BPDC occurs via a one-pot, two-step reductive amination. Since HQC is not able to cross-link chitosan on its own, glutaraldehyde (GA) was added. A schematic representation of the derivatization of chitosan is depicted in Fig. 2. All cross-linked compounds were analyzed using the following techniques: SEM, FTIR spectroscopy, XRPD analysis, TGA, elemental analysis, BET surface area analysis and point of zero charge determination. Secondary electron images were taken on a JEOL JSM-7600F FEG SEM apparatus. Gold sputtering was used prior to analysis. X-ray powder diffraction patterns were collected on a Thermo Scientific ARL X'Tra diffractometer, operated at 40 kV, 30 mA using Cu K α radiation ($\lambda = 1.5406 \text{ \AA}$). TA Netzsch Model STA 449 F3 Jupiter system was used to perform thermogravimetric analysis under N₂ flow (100 mL/min). For CHNS elemental analysis, a Thermo Flash 2000 thermal analyser (Thermo Scientific) is used with V₂O₅ as catalyst and methionine as standard. The specific Brunauer-Emmett-Teller (BET) surface area was measured on a TriStar 3000 analyser (Micromeritics) and a Belsorp Mini apparatus at 77 K. Prior to analysis, the samples were dried at 100°C under vacuum for 24 h. The pH at the point of zero charge (pH_{PZC}) of the products was determined in the pH range between 2 and 12.⁴³

Synthesis of 1,10-phenanthroline-2,9-dicarbaldehyde cross-linked chitosan (Ch-PDC) and [2,2'-bipyridine]-5,5'-dicarbaldehyde cross-linked chitosan (Ch-BPDC) Chitosan (1 eq., 1 g) was dissolved in 50 mL 1% (v/v) acetic acid (HOAc) at 50 °C for 1 h. Next, 0.4 eq. of chelating compound PDC or BPDC was added, together with a 1% (v/v) acetic acid solution to reduce the viscosity and to insure complete mixing (Entry 1 and 2, Table 4). The viscous mixture was stirred with an overhead stirrer at 50 °C for 4 h. Afterwards, 1.2 eq. of NaCNBH₃ (10 wt.% in H₂O) was added and stirred overnight at room temperature. The mixture was purified by dialysis in demineralized water for 5 days. The dialyzed solution was added to an excess of ethanol, which was consequently evaporated *in vacuo*. The resulting concentrated mixture was precipitated in acetone, centrifuged, filtered and washed with acetone. Finally, the product was dried in an oven at 60 °C overnight and resulted in PDC or BPDC cross-linked chitosan.

Table 4 Synthesis of chitosan biosorbents using different volumes of acetic acid solution (1% v/v HOAc)

Entry	Compound (concentration)	Volume HOAc (mL)
1	PDC (0.83% in DMSO)	60
2	BPDC (0.83% in DMSO)	125
3	HQC (1.25% in methanol)	25

Synthesis of glutaraldehyde cross-linked chitosan (Ch-GA) followed by grafting with 8-hydroxyquinoline-2-carbaldehyde (Ch-GA-HQC)

After the dissolution of chitosan in acetic acid, 0.2 eq of glutaraldehyde (GA 50% in H₂O) was added together with an extra amount of 1% HOAc solution (Entry 3, Table 4). After 1h, 0.4 eq. of HQC were added and the viscous mixture was stirred at 50 °C for 4 h. Afterwards, 1.2 eq. of NaCNBH₃ (10 wt.% in H₂O) was added and stirred overnight at room temperature and then purified as described above. Ch-GA was made without the addition of HQC, and using 0.4 eq. of NaCNBH₃ for the reduction. A lower amount of cross-linker was used compared to the synthesis of Ch-PDC and Ch-BPDC in order to have sufficient amine groups available for the modification with HQC.

Batch adsorption studies

Stock solutions of 1000 mg/L Pt and Pd were prepared by dissolving K₂PtCl₆ and PdCl₂ powder in 1.1 M HCl.⁵⁶ All other concentrations in the adsorption experiments were obtained by diluting the stock solution with deionized water to obtain a Pt(IV) or Pd(II) concentration in the range of 25 mg/L to 1000 mg/L. Batch adsorption experiments were performed in duplicate using 15 mL polyethylene tubes. A quantity of 10 mg of chitosan derivative (Ch-PDC, Ch-BPDC or Ch-GA-HQC) was added to 10 mL of a Pt and/or Pd solution. The initial pH was adjusted using 5 M NaOH or 0.2 M H₂SO₄. Then, the tubes were shaken at 200 rpm in a horizontal shaker at 20 ± 1 °C for a predetermined period of time (from 5 min to 24 h). After phase separation through sedimentation, the supernatant was filtered (MACHERY-NAGEL; CHROMAFIL® RC-45/25 syringe filter; pore size 0.45 μm) and analyzed using inductively coupled plasma optical emission spectroscopy (ICP-OES; Varian Vista MPX, Palo Alto, CA, USA). The adsorption efficiency (*A*%) and the amount

of Pt or Pd adsorbed per unit mass of the adsorbent, *q_t* (mg/g), at any time *t* (min) were calculated using the following equations (Eq. 1 and Eq. 2), in which *C₀* and *C_t* (mg/L) are the initial Pt(IV) or Pd(II) concentration and the concentration at time *t* (min), respectively. *V* (L) is the solution volume and *m* (g) is the adsorbent mass.

$$A\% = \left(\frac{C_0 - C_t}{C_0} \right) \times 100 \quad (\text{Eq. 1})$$

$$q_t = (C_0 - C_t) \left(\frac{V}{m} \right) \quad (\text{Eq. 2})$$

Effect of initial pH value The influence of pH was investigated at five different initial pH levels (1.0 ± 0.1 – 5.0 ± 0.1). Therefore, separate adsorbate solutions with a concentration of 25 mg/L were prepared as described above. After contacting for 24 h, the solution was analyzed for their Pt or Pd concentration.

Adsorption isotherms To determine the maximum sorption capacity for Pt and Pd adsorption, metal solutions with an initial concentration of 25 mg/L to 1000 mg/L were prepared at pH 3.0 ± 0.1 and analyzed after 24 h as described above. The experimental equilibrium data were evaluated using the Langmuir isotherm model (Eq. 3). In this model, *q_e* and *C_e* are the amount of Pd(II) or Pt(IV) adsorbed (mg/g) and the adsorbate concentration in the aqueous phase (mg/L), both at equilibrium. *q_m* (mg/g) and *K_L* (L/mg) are the Langmuir constants, which are related to the adsorption capacity and energy of adsorption, respectively. Both *q_m* and *K_L* were calculated by plotting *C_e* vs *q_e*, using the following equation.

$$q_e = \frac{q_m K_L C_e}{(1 + K_L C_e)} \quad (\text{Eq. 3})$$

The degree of suitability of the resin towards the metal ions was estimated from the values of the separation factor (*R_L*), which gives an indication for the possibility of the adsorption to proceed. *R_L* was calculated via Eq. 4, where *K_L* is the Langmuir equilibrium constant and *C₀* the initial concentration of Pt or Pd.

$$R_L = \frac{1}{1 + K_L C_0} \quad (\text{Eq. 4})$$

Adsorption kinetics Separate solutions of 25 mg/L Pt and Pd were prepared and the pH was adjusted to pH 3.0 ± 0.1. The samples were analyzed after different time intervals ranging from 5 min to 24 h, as described above. The experimental data were evaluated using non-linear form of pseudo-first-order and pseudo-second-order kinetics. This is because of non-linear regression method is more appropriate compared to linear method to determine the rate kinetic parameters.⁷³ The non-linear expressions of the pseudo-first-order and pseudo-second-order models are given in equations (5) and (6), respectively, in which *k₁* (min⁻¹) is the pseudo-first-order rate constant, *k₂* (g mg⁻¹ min⁻¹) is the pseudo-second-order rate constant, *q_t* and *q_e* are the adsorbed amount (mg/g) at any time *t* (min) and the adsorbed amount at equilibrium, respectively.

$$q_t = q_e (1 - \exp^{-k_1 t}) \quad (\text{Eq. 5})$$

$$q_t = \frac{k_2 q_e^2 t}{1 + k_2 q_e t_2} \quad (\text{Eq. 6})$$

Pore or internal diffusion was analyzed using the intra-particle diffusion model, given in Eq. 7.⁷⁴ In this model, q_t is the amount of Pt(IV) or Pd(II) adsorbed on the adsorbent (mg/g) at time t , k_p (mg/(g.min^{0.5})) is the intra-particle diffusion rate constant.

$$q_t = k_p \sqrt{t} \quad (\text{Eq. 7})$$

Regeneration of biosorbents Regeneration performances of the adsorbents was evaluated in three adsorption-desorption cycles. For the adsorption experiment, 10 mg of chitosan derivative was brought into contact with a 25 mg/L Pt(IV) or Pd(II) solution for 24 h. Then, the Pt or Pd loaded adsorbents were subjected to desorption by adding 10 mL of 0.25 M thiourea solution⁵⁶ in 15 mL polyethylene tubes and shaken at 200 rpm in a horizontal shaker for 24 h at 20 ± 1 °C. Then, the suspensions were filtered and the Pt or Pd content of the filtrate was measured. After rinsing with deionized water and drying at 70 °C for 24 h, the Pt and Pd adsorption efficiency of the regenerated adsorbents was determined in the next sorption cycle. All experiments were performed in duplicate.

Conclusions

In this paper, three new chitosan derivatives (Ch-PDC, Ch-BPDC and Ch-GA-HQC) were successfully prepared in line with the principles of green chemistry. The adsorption isotherms of Pd(II) and Pt(IV) were well described using the Langmuir model. The optimal level for precious metal adsorption was considered at pH 3, taking into account the chemical speciation. The modification of chitosan with HQC resulted in the highest adsorption capacity for both Pd and Pt, being 340.3 mg/g and 203.9 mg/g, respectively. Kinetic studies indicated that the adsorption follows pseudo-second-order kinetics, suggesting chemisorption as the main adsorption mechanism. The intra-particle diffusion model suggests that the sorption process occurs in two phases: external mass transfer is followed by an intra-particle diffusion process. The prepared adsorbents could be regenerated using mild conditions and reused in multiple adsorption/desorption cycles with recovery efficiencies above 95% for both elements. As the modification process significantly increased the adsorption capacity for Pt and Pd and made the materials stable under acid conditions and reusable, it can be concluded that there is a clear environmental gain of the functionalization process. This gain should be quantified by a complete life cycle assessment. Further study should focus on the performance and scalability of using the adsorbents on real waste streams in a continuous way.

Conflicts of interest

There are no conflicts to declare.

Acknowledgements

View Article Online

DOI: 10.1039/C9GC00166B

T. G. A. (BOF fellowship n°: 01W05414) is supported by Ghent University. Dr. Jonathan De Roo, prof. Isabel Van Driessche and Funda Aliç are warmly thanked for their guidance and help with the structural characterization measurements (TGA & CHNS). Further, the authors want to thank Pieter Naert for proofreading the manuscript and Yoshi Mertens and Jens Mincke for the graphical contribution.

Notes and references

- 1 A. Verlee, S. Mincke and C. V. Stevens, *Carbohydr. Polym.*, 2017, **164**, 268–283.
- 2 K. Kurita, *Prog. Polym. Sci.*, 2001, **26**, 1921–1971.
- 3 K. Kurita, *Mar. Biotechnol.*, 2006, **8**, 203–226.
- 4 S. Islam, M. A. R. Bhuiyan and M. N. Islam, *J. Polym. Environ.*, 2017, **25**, 854–866.
- 5 H. Wang, K. U. Rehman, X. Liu, Q. Yang, L. Zheng, W. Li, M. Cai, Q. Li, J. Zhang and Z. Yu, *Biotechnol. Biofuels*, 2017, **10**, 1–13.
- 6 A. Caligiani, A. Marseglia, G. Leni, S. Baldassarre, L. Maistrello, A. Dossena and S. Sforza, *Food Res. Int.*, 2018, **105**, 812–820.
- 7 Y.-S. Song, M.-W. Kim, C. Moon, D.-J. Seo, Y. S. Han, Y. H. Jo, M. Y. Hon, Y.-K. Park, S.-A. Kim, Y. W. Kim and W.-J. Jung, *Entomol. Res.*, 2017, **47**, 1–5.
- 8 P. Zou, X. Yang, J. Wang, Y. Li, H. Yu, Y. Zhang and G. Liu, *Food Chem.*, 2016, **190**, 1174–1181.
- 9 E. I. Rabea, M. E.-T. Badawy, C. V. Stevens, G. Smagghe and W. Steurbaut, *Biomacromolecules*, 2003, **4**, 1457–1465.
- 10 M. Rinaudo, *Prog. Polym. Sci.*, 2006, **31**, 603–632.
- 11 S. W. Won, P. Kotte, W. Wei, A. Lim and Y.-S. Yun, *Bioresour. Technol.*, 2014, **160**, 203–212.
- 12 F. Fu and Q. Wang, *J. Environ. Manage.*, 2011, **92**, 407–418.
- 13 R. Apiratikul and P. Pavasant, *Bioresour. Technol.*, 2008, **99**, 2766–2777.
- 14 T. H. Nguyen, C. H. Sonu and M. S. Lee, *Hydrometallurgy*, 2016, **164**, 71–77.
- 15 A. J. Hunt, T. J. Farmer and J. H. Clark, in *Element Recovery and Sustainability*, 2013, pp. 1–28.
- 16 A. Fornalczyk, *J. Achiev. Mater. Manuf. Eng.*, 2012, **55**, 864–869.
- 17 T. Kimuro, M. R. Gandhi, U. M. R. Kunda, F. Hamada and M. Yamada, *Hydrometallurgy*, 2017, **171**, 254–261.
- 18 K. Ravindra, L. Bencs and R. Van Grieken, *Sci. Total Environ.*, 2004, **318**, 1–43.
- 19 A. Lim, M.-H. Song, C.-W. Cho and Y.-S. Yun, *Appl. Sci.*, 2016, **6**, 12.
- 20 J. P. H. Perez, K. Folens, K. Leus, F. Vanhaecke, P. Van Der Voort and G. Du Laing, *Resour. Conserv. Recycl.*, 2019, **142**, 177–188.
- 21 L. Zhang, Y. Zeng and Z. Cheng, *J. Mol. Liq.*, 2016, **214**, 175–191.
- 22 A.-H. Chen, C.-Y. Yang, C.-Y. Chen, C.-Y. Chen and C.-W. Chen, *J. Hazard. Mater.*, 2009, **163**, 1068–1075.

- 23 K. Folens, A. Abebe, J. Tang, F. Ronsse and G. Du Laing, *Environ. Chem.*, 2018, **15**, 506.
- 24 A. J. Varma, S. V. Deshpande and J. F. Kennedy, *Carbohydr. Polym.*, 2004, **55**, 77–93.
- 25 W. S. Wan Ngah, C. S. Endud and R. Mayanar, *React. Funct. Polym.*, 2002, **50**, 181–190.
- 26 M. Rajiv Gandhi, G. N. Kousalya, N. Viswanathan and S. Meenakshi, *Carbohydr. Polym.*, 2011, **83**, 1082–1087.
- 27 V. E. Tikhonov, L. A. Radigina and Y. A. Yamskov, *Carbohydr. Res.*, 1996, **290**, 33–41.
- 28 E. R. Welsh and R. R. Price, *Biomacromolecules*, 2003, **4**, 1357–1361.
- 29 W. S. W. Ngah, S. Ab Ghani and A. Kamari, *Bioresour. Technol.*, 2005, **96**, 443–450.
- 30 T.-Y. Hsien and G. L. Rorrer, *Ind. Eng. Chem. Res.*, 1997, **36**, 3631–3638.
- 31 Y. Koyama and A. Taniguchi, *J. Appl. Polym. Sci.*, 1986, **31**, 1951–1954.
- 32 M. J. Woolley, G. N. Khairallah, G. da Silva, P. S. Donnelly, B. F. Yates and R. A. J. O’Hair, *Organometallics*, 2013, **32**, 6931–6944.
- 33 N. Lu, Y.-J. Lu, J.-Y. Huang, H.-F. Chiang, C.-C. Kung, Y.-S. Wen and L.-K. Liu, *J. Chinese Chem. Soc.*, 2018, **65**, 613–627.
- 34 B. Côté and G. P. Demopoulos*, *Solvent Extr. Ion Exch.*, 1994, **12**, 393–421.
- 35 B. Côté and G. P. Demopoulos, *Solvent Extr. Ion Exch.*, 1994, **12**, 517–540.
- 36 M. Ruiz, A. M. Sastre and E. Guibal, *React. Funct. Polym.*, 2000, **45**, 155–173.
- 37 J. Kumirska, M. Czerwicka, Z. Kaczyński, A. Bychowska, K. Brzozowski, J. Thöming and P. Stepnowski, *Mar. Drugs*, 2010, **8**, 1567–1636.
- 38 P. Nagaraj, A. Sasidharan, V. David, A. Sambandam, P. Nagaraj, A. Sasidharan, V. David and A. Sambandam, *Polymers (Basel)*, 2017, **9**, 667.
- 39 M. Monier, D. A. Abdel-Latif and Y. G. Abou El-Reash, *J. Colloid Interface Sci.*, 2016, **469**, 344–354.
- 40 I. Corazzari, R. Nisticò, F. Turci, M. G. Faga, F. Franzoso, S. Tabasso and G. Magnacca, *Polym. Degrad. Stab.*, 2015, **112**, 1–9.
- 41 P.-Z. Hong, S.-D. Li, C.-Y. Ou, C.-P. Li, L. Yang and C.-H. Zhang, *J. Appl. Polym. Sci.*, 2007, **105**, 547–551.
- 42 X. Ju, K. Igarashi, S. Miyashita, H. Mitsuhashi, K. Inagaki, S. Fujii, H. Sawada, T. Kuwabara and A. Minoda, *Bioresour. Technol.*, 2016, **211**, 759–764.
- 43 A. Padilla-Rodríguez, J. A. Hernández-Viezcás, J. R. Peralta-Videa, J. L. Gardea-Torresdey, O. Perales-Pérez and F. R. Román-Velázquez, *Microchem. J.*, 2015, **118**, 1–11.
- 44 L. Zhou, J. Liu and Z. Liu, *J. Hazard. Mater.*, 2009, **172**, 439–446.
- 45 S. A. Johannessen, B. O. Petersen, J. Duus and T. Skrydstrup, *Inorg. Chem.*, 2007, **47**, 4326–4335.
- 46 S. Sharma, A. S. Krishna Kumar and N. Rajesh, *RSC Adv.*, 2017, **7**, 52133–52142.
- 47 L. Zhou, J. Xu, X. Liang and Z. Liu, *J. Hazard. Mater.*, 2010, **182**, 518–524.
- 48 P. Chassary, T. Vincent, J. Sanchez Marciano, L. E. Macaskie and E. Guibal, *Hydrometallurgy*, 2005, **76**, 131–147.
- 49 K. Folens, S. Van Hulle, F. Vanhaecke and G. Du Laing, *Water Sci. Technol.*, 2016, **73**, 1738–1745.
- 50 C. Colombo, C. J. Oates, A. J. Monhemius and J. A. Plant, *Geochemistry Explor. Environ. Anal.*, 2008, **8**, 91–101.
- 51 K. Fujiwara, A. Ramesh, T. Maki, H. Hasegawa and K. Ueda, *J. Hazard. Mater.*, 2007, **146**, 39–50.
- 52 W. A. Spieker, J. Liu, J. T. Miller, A. J. Kropf and J. R. Regalbuto, *Appl. Catal. A Gen.*, 2002, **232**, 219–235.
- 53 S. Döker, S. Malcı, M. Doğan and B. Salih, *Anal. Chim. Acta*, 2005, **553**, 73–82.
- 54 K. Folens, K. Leus, N. R. Nicomel, M. Meledina, S. Turner, G. Van Tendeloo, G. Du Laing and P. Van Der Voort, *Eur. J. Inorg. Chem.*, 2016, **2016**, 4395–4401.
- 55 S. Nagireddi, V. Katiyar and R. Uppaluri, *Int. J. Biol. Macromol.*, 2017, **94**, 72–84.
- 56 D. Sicupira, K. Campos, T. Vincent, V. Leao and E. Guibal, *Adsorption*, 2010, **16**, 127–139.
- 57 E. Guibal, N. Von Offenbergy Sweeney, M. Zikan, T. Vincent and J. Tobin, *Int. J. Biol. Macromol.*, 2001, **28**, 401–408.
- 58 S. Wang, T. Vincent, J.-C. Roux, C. Faur and E. Guibal, *Chem. Eng. J.*, 2017, **313**, 567–579.
- 59 P. K. Malik, *J. Hazard. Mater.*, 2004, **113**, 81–88.
- 60 H. Sharifard, M. Soleimani and F. Z. Ashtiani, *Int. J. Glob. Warm.*, 2014, **6**, 303.
- 61 A. Ramesh, H. Hasegawa, W. Sugimoto, T. Maki and K. Ueda, *Bioresour. Technol.*, 2008, **99**, 3801–3809.
- 62 X. Zhang, S. Ding, Y. Wang, X. Feng, Q. Peng and S. Ma, *J. Appl. Polym. Sci.*, 2006, **100**, 2705–2709.
- 63 E. Guibal, N. Von Offenbergy Sweeney, T. Vincent and J. M. Tobin, *React. Funct. Polym.*, 2002, **50**, 149–163.
- 64 S. Sharma and N. Rajesh, *J. Environ. Chem. Eng.*, 2017, **5**, 1927–1935.
- 65 M. P. Di Bello, M. R. Lazoi, G. Mele, S. Scorrano, L. Mergola and R. Del Sole, *Materials (Basel)*, 2017, **10**, 16.
- 66 Q. Xie, T. Lin, F. Chen, D. Wang and B. Yang, *Hydrometallurgy*, 2018, **178**, 188–194.
- 67 E. I. Kapitanova, A. A. Ibragimova, Y. S. Petrova, A. V. Pestov and L. K. Neudachina, *Russ. J. Appl. Chem.*, 2018, **91**, 297–303.
- 68 E. Guibal, A. Larkin, T. Vincent and T. John Michael, *Ind. Eng. Chem. Res.*, 1999, **38**, 4011–4022.
- 69 M.-H. Song, S. Kim, D. H. K. Reddy, W. Wei, J. K. Bediako, S. Park and Y.-S. Yun, *J. Hazard. Mater.*, 2017, **324**, 724–731.
- 70 C. Ruan, M. Strømme and J. Lindh, *Cellulose*, 2016, **23**, 2627–2638.
- 71 B. C. Choudhary, D. Paul, A. U. Borse and D. J. Garole, *J. Chem. Technol. Biotechnol.*, 2017, **92**, 1667–1677.
- 72 N. Azizi, A. Khajeh-Amiri, H. Ghafari and M. Bolourtchian, *Mol. Divers.*, 2011, **15**, 157–161.
- 73 K. V. Kumar, *J. Hazard. Mater.*, 2006, **137**, 1538–1544.
- 74 N. Viswanathan, C. Sairam Sundaram and S. Meenakshi, *J. Hazard. Mater.*, 2009, **167**, 325–331.